



Grain and crystallite size evaluation of cryomilled pure copper

M. Samadi Khoshkhoo^{a,*}, S. Scudino^a, J. Thomas^a, K.B. Surreddi^a, J. Eckert^{a,b}

^a IFW Dresden, Institut für Komplexe Materialien, Postfach 27 01 16, D-01171 Dresden, Germany

^b TU Dresden, Institut für Werkstoffwissenschaft, D-01062 Dresden, Germany

ARTICLE INFO

Article history:

Received 2 July 2010

Received in revised form 18 January 2011

Accepted 14 February 2011

Available online 21 February 2011

Keywords:

Nanostructured materials

Mechanical alloying

X-ray diffraction

Transmission electron microscopy, TEM

ABSTRACT

The crystallite and grain sizes of pure copper milled at cryogenic temperature for different periods have been characterized using X-ray diffraction (XRD) and transmission electron microscopy (TEM). X-ray line profile analysis using a modified Williamson–Hall method [T. Ungár, Á. Révész, A. Borbély, J. Appl. Crystallogr. 31 (1998) 554], which takes into account the strain anisotropy induced by dislocations and planar faults, was used to determine the size of the coherently scattering domains. The results reveal that the modified Williamson–Hall method leads to values that are in very good agreement with the data obtained by TEM, in particular when considering the effect of planar faults.

© 2011 Elsevier B.V. All rights reserved.

1. Introduction

Nanocrystalline materials with particle or grain sizes, layer thicknesses, or coherent domain sizes in the nanometer range (typically less than 100 nm at least in one dimension) have been attracting increasing attention in the last years due to their remarkable physical and chemical properties that may significantly differ from those of the corresponding coarse-grained materials with the same composition [1–3]. Characterizing a nanostructure is a challenging task. The most problematic issue is the determination of grain size and grain size distribution [4,5]. Size and strain analysis based on X-ray diffraction (XRD) is the most common method for the evaluation of the coherently scattering domain size in nanocrystalline materials [4–8]. The method is an indirect approach and is based on the broadening of the X-ray reflections [8,9]. On the other hand, grain size determination by TEM is based on the direct observation of the microstructure [4]. As a result, a rather large discrepancy is generally observed between the grain size observed by XRD and TEM [5].

The observed size discrepancy between XRD and TEM analysis can be ascribed to the fact that XRD gives the mean size of the crystallites or coherently scattering domains (i.e. the smallest unfaulted portion of the crystal [10]), while TEM observations take into account the grains, which can be defined as the region of a polycrystalline material with the same crystallographic orientation and same structure [11]. When nanocrystalline materials are produced by methods like inert gas condensation or electrodeposition,

the values obtained by both XRD and TEM are in good agreement [10,12]. However, in most of the materials grains and coherently scattering domains are not coinciding. This is particularly true in the case of materials formed by severe plastic deformation (SPD). In these materials, the structure actually consists of substructures: grains (separated by high angle grain boundaries) and sub-grains/dislocation cells (separated by low angle grain boundaries) [10,12]. The difference between the spatial orientation of these substructures is small (typically 1–2°) and it does not induce any visible contrast in normal TEM investigations [12]. However, such a difference in orientation is large enough for breaking down the coherent scattering. Therefore, there is a phase shift between the X-rays diffracted from different substructures inside a single grain [12]. The line profile of a grain is the sum of the line profiles of the substructures and, as a result, the size information obtained by XRD is related to sub-grains/dislocation cells (grain sub-structures). In addition, it has been shown that during the SPD process, a special dislocation structure, i.e. dislocation dipoles, can form [12]. The two crystal halves on each side of the dipolar dislocation walls do not have any difference in orientation. Therefore, there is no contrast in TEM images. However, this dislocation structure can break down the coherent scattering, contributing to the observed discrepancy between the size information obtained by TEM and XRD [12].

Recently, Ungár et al. [13,14] have developed a new model for the precise determination of the crystallite size of SPD metals using XRD. This model is a modification of the classical Williamson–Hall method that takes into account the effect of the anisotropy of peak broadening as a function of the diffraction order, i.e. the line broadening does not increase monotonically with the order of reflections [13,14]. The model considers the strain anisotropy due to

* Corresponding author. Tel.: +49 351 4659 747; fax: +49 351 4659 452.
E-mail address: m.samadi.khoshkhoo@ifw-dresden.de (M.S. Khoshkhoo).

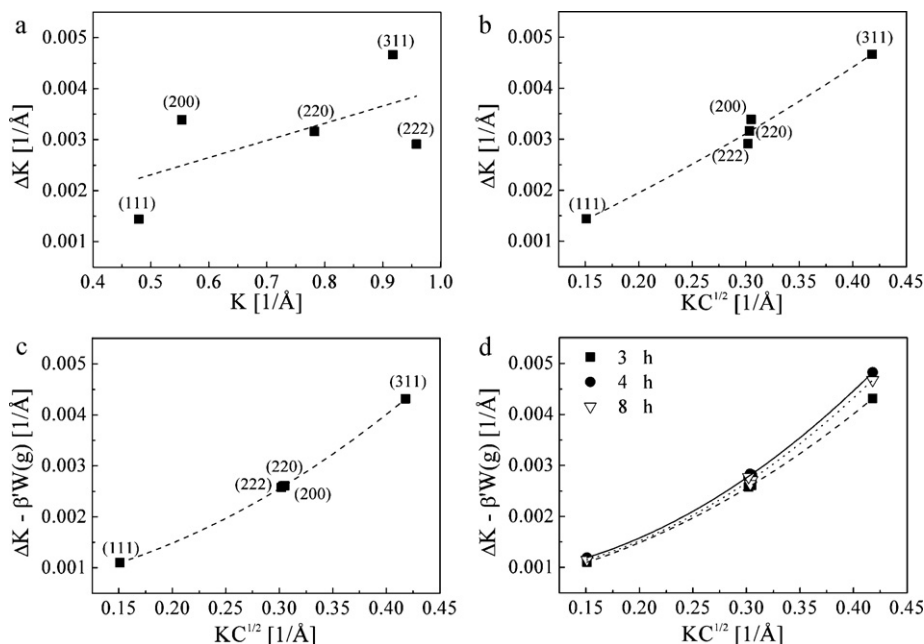


Fig. 1. (a) Classical Williamson–Hall plot, (b) modified Williamson–Hall plot considering dislocation-induced strain anisotropy, (c) Williamson–Hall plot considering dislocation-induced strain anisotropy and the effect of planar faults, for pure Cu milled for 3 h and (d) modified Williamson–Hall plot for the samples milled for different periods.

dislocations and also considers planar faults, and introduces correction parameters to restore the monotonic behavior [13,14].

In this work, the modified Williamson–Hall method developed by Ungár et al. [13,14] have been used to monitor the evolution of the coherently scattering domain size of pure copper during milling at cryogenic temperature. The results have been compared to the grain size evaluated by TEM, revealing a good agreement with the data obtained by the different methods.

2. Experimental details

Milling experiments starting from pure copper powder (purity > 99.99 wt.%) were performed using a Retsch PM400 planetary ball mill and hardened steel balls and vials. The powders were milled up to 8 h with a ball-to-powder mass ratio (BPR) of 10:1 and a milling intensity of 400 rpm. To keep the vial temperature at cryogenic regime, milling was carried out as a sequence of cooling–milling intervals: the vial was cooled down in liquid nitrogen bath for 1 h and then milling was performed for 15 min to avoid a strong temperature rise. This process was repeated to reach the desired milling time. To avoid or minimize possible atmosphere contamination during milling, vial charging and any subsequent sample handling was carried out in a glove box under purified argon atmosphere (less than 1 ppm O₂ and H₂O). Microstructural characterization was performed using transmission electron microscopy and X-ray diffraction techniques. For TEM, bulk small flakes obtained by ball milling were grinded to around 100 μm and then dimple grinded using a GATAN dimple grinding machine. As the final step ion milling using a GATAN-PIPS ion milling machine was used to remove all mechanical effects introduced by sample preparation methods. A Philips CM-20 transmission electron microscope operating at 200 kV was used to evaluate the microstructure. The average grain sizes and grain size distributions were obtained by TEM through the measurement of more than 1100 grains in bright- and dark-field images. XRD experiments were done in transmission geometry using a STOE Stadi P diffractometer (Cu-Kα₁ radiation) operating at 40 kV with small instrumental broadening. A curved Ge (1 1 1) crystal monochromator was used for the purification of the X-ray beam from Kα₂ radiation. The diffraction patterns were recorded using a linear position sensitive detector with the 2-theta (diffraction angle) range of 6°. For the modified Williamson–Hall method, a polycrystalline copper specimen annealed for 16 h at 600 °C, was used to determine the values of instrumental broadening exactly at the 2-theta positions of the XRD reflections.

3. Results and discussion

The classical Williamson–Hall method permits to evaluate the individual effects of size and strain from the total amount of line

broadening as [8]:

$$\frac{2 \cos \theta (\Delta\theta)}{\lambda} = \frac{c}{d} + \frac{2\varepsilon \sin \theta}{\lambda} \quad (1)$$

where ε represents the broadening resulting from strain, d is the mean size of the coherently scattering domain, $\Delta\theta$, λ and θ are the full width at half maximum (FWHM), X-ray wavelength and the diffraction angle, respectively, and c is a constant typically taken as 0.9 [13].

Eq. (1) can be simplified as:

$$\Delta K = \frac{0.9}{d} + \varepsilon K \quad (2)$$

with $K = 2 \sin \theta / \lambda$ and $\Delta K = 2 \cos \theta (\Delta\theta) / \lambda$. Thus, a plot of ΔK versus K should give a straight line of gradient ε and intercept $1/d$. As a typical example of this method, Fig. 1(a) displays the values of ΔK for the powder milled for 3 h as a function of K . The plot clearly shows that the line broadening is not a monotonic function of K , as already observed for ultrafine grained and nanocrystalline metals [13,14]. This is because the Williamson–Hall method does not consider the strain anisotropy [8], which is typical of the dislocated (deformed) materials [10]. As a result, no reliable values of d were obtained using this approach for the present milled samples.

The main strain contribution to line broadening comes from dislocations [10]. The non-monotonic variation of the line broadening with the order of reflections (i.e. the strain anisotropy) can be explained by considering the contribution of dislocations as orientation-dependent, in a similar way as the contrast of dislocations in electron microscopy [10]. The anisotropic effect of dislocations can be described by the average contrast factor of dislocations \bar{C} , which depends on the particular reflection considered [13]. This contribution to line broadening can be taken into account by modifying Eq. (2) as [13]:

$$\Delta K = \frac{0.9}{d} + \left(\frac{\pi A b^2}{2} \right)^{1/2} \rho^{1/2} (K \bar{C}^{1/2}) + \left(\frac{\pi A' b^2}{2} \right)^{1/2} Q^{1/2} (K^2 \bar{C}) \quad (3)$$

where A and A' are parameters determined by the effective outer cutoff radius of dislocations, b is the Burgers vector, ρ is the

Table 1

Crystallite and grain sizes of cryomilled pure Cu evaluated by the modified Williamson–Hall method and by TEM.

Milling time (h)		3	4	8
Crystallite size (nm)	Modified Williamson–Hall equation (3)	888 ^a	804 ^a	486 ^a
	Modified Williamson–Hall equation (4)	176 ± 12	112 ± 13	113 ± 47
Grain size (nm)	TEM	144 ± 70	128 ± 57	111 ± 50

^a In this case the error was larger than the calculated size value.

dislocation density and Q is the correlation term of the dislocation system [13]. Fig. 1(b) shows the values of ΔK for the powder milled for 3 h plotted as a function of $K\bar{C}^{1/2}$. The values of C , calculated on the assumption that half of the dislocations are of screw type and half are of edge type, were taken from [13]. The results reveal that improved dependence of the breadth on the diffraction vector can be obtained by taking into account the strain anisotropy through the dislocation contrast factor. In contrast to the classical Williamson–Hall plot, where ΔK scales with K , the scaling factor for the modified Williamson–Hall approach in Eq. (3) is $K\bar{C}^{1/2}$. Therefore, a second order polynomial fit was used to determine the size of the coherently scattering domains. The results, summarized in Table 1, indicate that the crystallite size decreases from 888 nm for the powder milled for 3 h to 486 nm for the material milled for 8 h.

Plastic deformation of fcc metals, such as Cu, produces planar faults (as shown in Fig. 2(a) for the present cryomilled powder) and other lattice defects whose density increases with increasing the amount of deformation [15]. Beside the deformation planar faults, the structure also contains the grown-in planar faults that have been developed during the production process of the material. These planar faults lead to both inhomogeneous shift and broadening of the XRD reflections [15]. It has been shown that the presence of planar faults increases the size contribution to the line broadening and, as a result, the apparent coherently scattering domain size is reduced [10,16].

The effect of planar faults can be considered by modifying Eq. (3) as [14]:

$$\Delta K - \beta'W(g) = \frac{0.9}{d} + \left(\frac{\pi Ab^2}{2}\right)^{1/2} \rho^{1/2}(K\bar{C}^{1/2}) + \left(\frac{\pi A'b^2}{2}\right)^{1/2} \rho^{1/2}(K^2\bar{C}), \quad (4)$$

where $W(g)$ is a factor that takes into account the order dependence of the effect of planar faults on the size contribution to the broadening, β' is the frequency of the planar faults and is equal to $(1.5\alpha + \beta)/a$, where α and β are the densities of stacking and twinning faults, respectively and a is the lattice constant [14].

The values of $\Delta K - \beta'W(g)$ for the powder milled for 3 h plotted as a function of $K\bar{C}^{1/2}$ with β' ranging between 0.00068 and 0.00123 (calibrated from fitting) and with $W(g)$ taken from [17] are shown in Fig. 1(c). The results clearly indicate that by taking into account the anisotropic effects of dislocations and planar faults, the line broadening increases monotonically with the order of the reflections. This is further corroborated by Fig. 1(d), which summarizes the values of $\Delta K - \beta'W(g)$ versus $K\bar{C}^{1/2}$ for the powders milled for different periods. The resulting variation of the crystallite size as a function of the milling time are shown in Table 1, revealing that the size decreases from 176 nm for the powder milled for 3 h to 113 nm for the material milled for 8 h.

The evolution of the grain size during milling was also monitored by TEM. Fig. 3 shows typical TEM micrographs of the powder milled for different periods along with the corresponding grain size distributions. The size distribution is rather broad for all of the milled samples. Especially, the sample milled for 3 h (Fig. 3(a)) displays a grain size ranging between 50 and 400 nm. With increasing

the milling time, the size distribution becomes slightly narrower by the disappearance of the larger grains (>300 nm) and, finally, for the sample milled for 8 h (Fig. 3(c)), the grain size ranges between 30 and 300 nm. These findings indicate that the microstructure of the milled powders consists of a mixture of both nc and ufg grains. The values of the mean grain size evaluated from Fig. 3 are presented in Table 1. The grain size decreases with increasing the milling time from 144 nm for the powder milled for 3 h to about 111 nm after 8 h of milling. This trend is very similar to what observed by the modified Williamson–Hall method.

The similarity between grain size observed by TEM and the size of the coherently scattering domain evaluated by Eq. (4) is

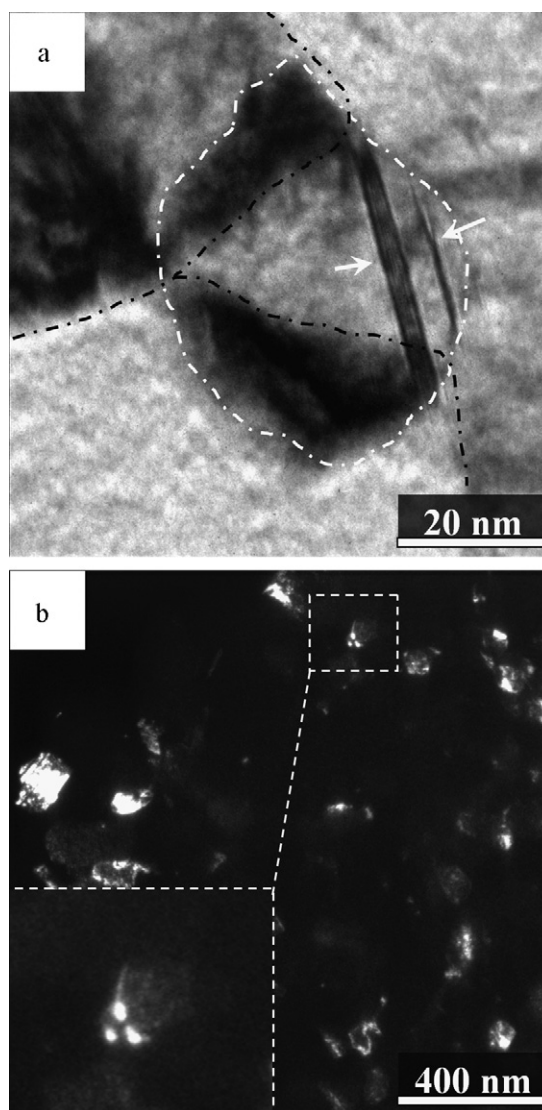


Fig. 2. TEM micrographs of cryomilled pure Cu showing (a) example of overlapping grains (dashed and dotted lines) and planar faults (indicated by arrows), and (b) object which can be considered as a distorted single grain as well as a group of three different grains.

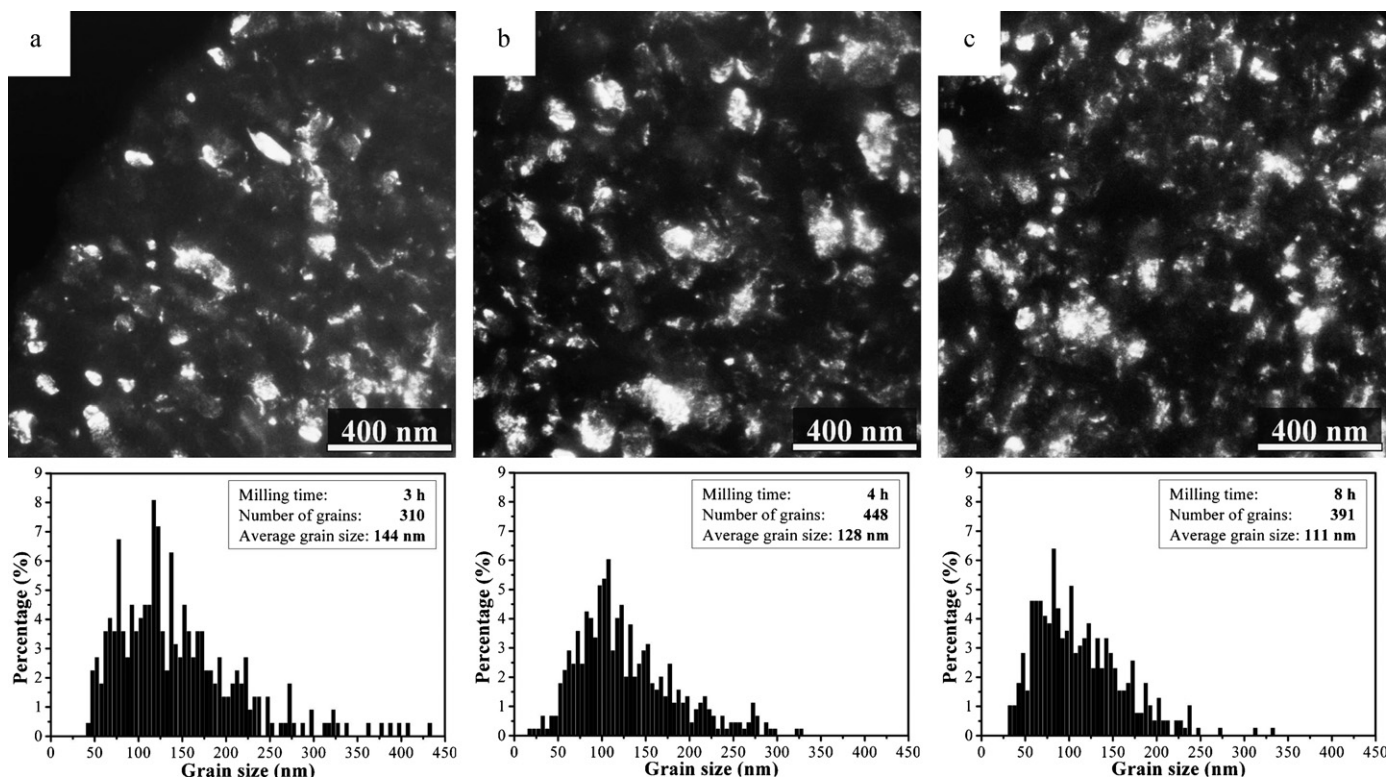


Fig. 3. Dark field TEM micrographs of pure Cu powder milled for (a) 3, (b) 4 and (c) 8 h and corresponding grain size distributions.

rather unusual. In fact, considering the intrinsic differences characterizing the grain size and the crystallite size for SPD materials already mentioned in Section 1, the size values obtained by XRD should be always smaller than those observed by TEM. This aspect can be understood by considering that the sizes obtained by the modified Williamson–Hall method are volume weighted values, whereas TEM gives the area weighted grain sizes. As reported by Langford et al. [18], for an existing size distribution, the volume weighted mean size is always higher than the area weighted size. Therefore, if the volume weighted data obtained by the modified Williamson–Hall method (Eqs. (3) and (4)) are converted to area weighted values, they should be smaller than the values obtained by TEM. With increasing the amount of plastic deformation, the dislocation density increases and, as a result, the low-angle sub-grain or cell boundaries will be converted to high angle grain boundaries and the result of the two methods will become more similar [12]. For the present case, the low temperature used for the cryomilling experiments most likely leads to an increased dislocation density due to reduced recovery processes at this temperature and thus the similarity of the results between the two methods of size determination is expected to be more pronounced.

Finally, an aspect that should be considered in the comparison of grain and crystallite sizes is the possible overestimation of the grain size by TEM analysis. This overestimation may arise from the fact that very small grains can be easily ignored in TEM investigations of the highly distorted materials. Grain size evaluation by TEM is based on the direct observation of the grains. Although in principle this approach should provide the most accurate size estimation, several aspects may affect the appearance of each individual grain in the TEM micrographs, which, in turn, may influence the final results. A typical example is given by lattice defects and distortions. In a crystal with low density of defects each single grain can be easily distinguished by diffraction contrast [19]. However, when the crystal structure undergoes a large amount of deformation, as in the present mechanically milled

powders, grains are highly bended and distorted and they have a high inhomogeneous internal strain [20]. Because of bending and distortion, the Bragg condition is not fulfilled at the same time across a single grain. Thus, only a certain part of a single grain which fulfills the Bragg condition gives diffraction contrast and will be visible. Partial overlapping of different grains along the sample thickness makes the situation even more complex, because the determination of the boundaries of a single grain becomes increasingly difficult, as shown in Fig. 2(a). Therefore, deciding what is being observed is a single grain, a distorted part of a single grain or the superimposition of more grains becomes extremely difficult, in particular during inspection of TEM micrographs with low magnifications, which are generally used to reach good statistics. An example of this situation is shown in Fig. 2(b), showing an object which can be considered as a distorted single grain as well as a group of three different grains. This introduces a high degree of uncertainty in the grain size evaluation by TEM. To avoid this problem, in this work, such grains were disregarded and were not considered for grain size evaluation. Of course, such a selection of grains for the grain size evaluation may easily lead to an overestimation of the mean size, consequently shifting the size distribution towards larger sizes (Fig. 2).

4. Conclusions

In this work, X-ray line profile analysis using a modified Williamson–Hall method was used for evaluation of the coherently scattering domains of nanostructured copper produced by cryomilling. This method takes into account the effect of the anisotropy of peak broadening as a function of the order of reflections induced by dislocations, and also considers the effect of planar faults and introduces correction parameters to restore the monotonic behavior. The results further demonstrate this method offers an effective tool for the precise determination of the crystallite size of severely deformed fcc metals.

Acknowledgements

The authors thank H. Schulze and U. Wilke for technical assistance, and F. Ali, M. Sakaliyska, H. Ehrenberg, F.A. Javid, O. Khvostikova and U. Kühn for stimulating discussions. This work was supported by the Deutsche Forschungsgemeinschaft (DFG), the National Science Foundation (NSF) and the Nationale Forschungsnetzwerke (NFN). K.B. Surreddi is grateful for the financial support provided by the DAAD.

References

- [1] H. Gleiter, *Prog. Mater. Sci.* 33 (1989) 223–315.
- [2] J. Eckert, J.C. Holzer, C.E. Krill III, W.L. Johnson, *J. Mater. Res.* 7 (1992) 1751.
- [3] C.C Koch, *Nanostructured Materials: Processing, Properties and Potential Applications*, Noyes Publications, William Andrew Publishing, Norwich NY, 2002.
- [4] J. Guerrero-Paz, D. Jaramillo-Vigueras, *Nanostruct. Mater.* 11 (1999) 1195.
- [5] Y. Zhong, D.H. Ping, X.Y. Song, F.X. Yin, *J. Alloys Compd.* 476 (2009) 113.
- [6] A. Dubravina, M.J. Zehetbauer, E. Schafner, I.V. Alexandrov, *Mater. Sci. Eng. A* 387–389 (2004) 817.
- [7] E. Schafner, G. Steiner, E. Korznikova, M. Kerber, M.J. Zehetbauer, *Mater. Sci. Eng. A* 410–411 (2005) 169.
- [8] G.K. Williamson, W.H. Hall, *Acta Metall.* 1 (1953) 22.
- [9] H.M. Rietveld, *J. Appl. Crystallogr.* 2 (1969) 65.
- [10] E. Schafner, M. Zehetbauer, *Rev. Adv. Mater. Sci.* 10 (2005) 28.
- [11] J.H. Oh, E.H. Kim, D.H. Kang, J. h. Cheon, K.H. Kim, J. Jang, *Thin Solid Films* 515 (2007) 5054.
- [12] T. Ungár, G. Tichy, J. Gubicza, R.J. Hellmig, *Powder Diffr.* 20 (2005) 366.
- [13] T. Ungár, A. Borbély, *Appl. Phys. Lett.* 69 (1996) 3173.
- [14] T. Ungár, Á. Révész, A. Borbély, *J. Appl. Crystallogr.* 31 (1998) 554.
- [15] M.S. Paterson, *J. Appl. Phys.* 23 (1952) 805.
- [16] B.E. Warren, *Prog. Met. Phys.* 8 (1959) 147.
- [17] T. Ungár, S. Ott, P.G. Sanders, A. Borbély, J.R. Weertman, *Acta Mater.* 46 (1998) 3693.
- [18] J.I. Langford, D. Louer, P. Scardi, *J. Appl. Crystallogr.* 33 (2000) 964.
- [19] D.B. Williams, C.B. Carter, *Transmission Electron Microscopy: A Textbook for Materials Science*, Plenum Publishing Corporation, New York, 1997.
- [20] S. Gomari, S. Sharafi, *J. Alloys Compd.* 490 (2010) 26.